Cr_3C_2-Ni-Cr coating properties of HVOF-YAG hybrid spraying and its strengthening mechanism†

KUWASHIMA Takayuki *, TAKAHASHI Ikuo*, TOMITA Tomoki**, OHMORI Akira ***

Abstract

Although thermal spraying technique is used in many industries, it suffers from several problems. For example, the hardness of the coatings is lower than that of sintered materials with incomplete cohesiveness. An yttrium aluminum garnet (YAG) laser was used during HVOF spraying to improve the properties of the applied coating. Cr_3C_2-Ni-Cr powder was used as thermal spray material, and stainless steel (SUS304) used as substrate. Coatings were sprayed by a hybrid spraying method, which was combined HVOF spraying with YAG laser. The hardness of coatings sprayed by hybrid spraying was higher and the weight loss in a blast-erosion test was smaller than that of coatings applied by HVOF spraying only. The particles deposited in the coatings obtained by hybrid spraying were very fine. Laser irradiation applied to the HVOF flame improved the adhesion strength between particles and the deposition of fine carbide particles in the coating. It was considered that mechanism of coating strengthening in hybrid spraying resulted from strengthening of cohesiveness by heating effects and decreasing of porosity by flattening effects according to observation results of Ni splats sprayed by the hybrid spraying method.

KEY WORDS: (HVOF spraying)(YAG laser)(Hybrid spraying)(cohesive strength)(blast erosion)(splat)

1. Introduction

For the advantages of higher hardness, fewer pores as well as tight bonding strengths with substrates of carbide cermets, coatings such as WC-Co and Cr_3C_2-Ni-Cr are sprayed by high-velocity oxy-fuel spraying methods, and are widely utilized in many application fields, such as calendaring rolls at steel mills and so on [1-3]. Comparing with the WC-Co coating, Cr_3C_2-Ni-Cr coatings are widely applied for heat-treatment rolls installed inside boilers or for various processes in steel mills due to their superior abrasion resistance at high temperature and are also used in other applications such as structural materials used in high temperature environments.

However, in this coating formation processes of thermal spraying, the following points should be considered. (1) The cohesive forces between coating and adhesive and between coating and substrate are mainly mechanical bonding originating in the coating forming process, (2) Deformation of the substrate should be considered in the process of coating reinforcement by heat-treatment, (3) coatings have lots of pores, which have inferior abrasion resistance compared with that of sintered ones [4-5].

In this attempt, the authors have developed a hybrid thermal spray coating method [5], which is the combination of conventional high-velocity oxy-fuel spray coating (High Velocity Oxy-Fuel Spraying Process, hereinafter referred as HVOF) and additional YAG laser irradiation for the fabrication of carbide cermet coatings [6]. This research has focused mainly on the laser irradiation assisting effect on the coating formation and on coating formation mechanism by applying the HVOF-YAG laser hybrid thermal spray method on Cr_3C_2-Ni-Cr cermet coatings (Hereafter, carbide cermet is referred to simply as cermet), which are highly desirable as abrasion resistance coatings in high temperature environments.

2. Experimental Method

2.1 Test specimen

The feedstock powders were commercially available Cr_3C_2-16Ni-4Cr (size10~45um). Pure nickel powder was used in order to examine the effect of laser power in hybrid spraying by observing the splat shape. **Fig.1** shows SEM photographs of morphology of spray

† Received on November 30, 2004
* Iwate Industrial Research Institute
** Hyogo Prefectural Institute of Industrial Research
*** Professor

Transactions of JWRI is published by Joining and Welding Research Institute of Osaka University, Ibaraki, Osaka 567-0047, Japan

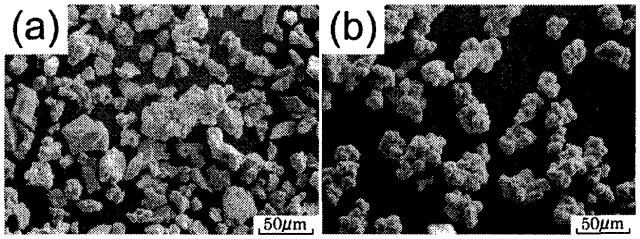

Fig.1 SEM photographs of spray materials.
(a) Cr_3C_2-Ni-Cr , (b) Ni

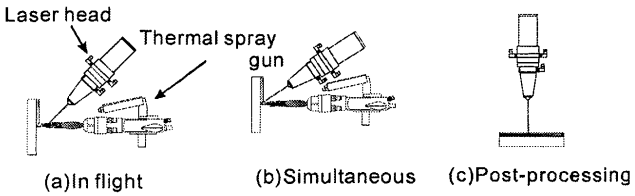

Fig.2 Schematic diagram of the combination methods of laser irradiation with HVOF spraying.

materials. Cr_3C_2-Ni-Cr powder was cladding powder [7]. SUS304 steel (Size: 50mm x 60mm x 5mm) was used as substrate in this experiment, and it was cleaned with acetone and blasted by alumina before thermal spraying.

2.2Combination methods of Laser and HVOF spraying

There are several combination methods of laser and HVOF spraying. **Fig.2** shows a schematic diagram of the combination methods of laser irradiation with HVOF spraying. **Fig.2**(a) and (b) were simultaneous laser irradiation on HVOF spraying methods(hybrid spraying method). In-flight particles were irradiated by laser as shown in **Fig.2**(a) and impacted particles on the substrate were irradiated laser as shown in **Fig.2**(b). **Fig.2**(c) was a laser treatment after HVOF spraying (after laser treatment method). **Fig.2**(a) method is difficult to realize because high laser power is required for high in-flight particle velocities. In this study, hybrid sprayed coating properties were investigated and its coating strengthening mechanism was examined by observation of splat shape.
For the implementation of this experiment, high velocity flame spraying equipment (DJ thermal spraying system, Sulzer Metco) was used and propylene-oxygen was used as fuel gas. As the laser excitation equipment, a YAG laser system with maximum output of 3kW (Ishikawajima-Harima Ltd. Model iLS-YC25C) was used.

Fig.3 and **Fig.4** show the photograph and schematic diagram of the hybrid spraying system. The spray parameters of HVOF and laser irradiation conditions are listed in **Table 1**. A combination of thermal spraying gun and laser head were installed at the specified distance from the test piece so that the flame from thermal spray gun and laser beam from the laser head could meet crosswise on the surface of the substrate. In the next stage the jig holding the test piece in position has to be mounted onto a six axis multiarticular robot,

Table 1 HVOF spray condition and Hybrid spray condition.

Oxygen	Pressure(MPa)	1.026
	Flow rates(L/min)	318
Propylene	Pressure(MPa)	0.684
	Flow rates(L /min)	66
Air	Pressure(MPa)	0.479
	Flow rates(L /min)	307
Spray distance(mm)		225
Traverse speed(mm/s)		200
Powder feeding rates(g/min)		30
Coating thickness(μ m)		200
Laser power(kW)		0,1.5,2.0,2.5
Defocus distance(mm)		60

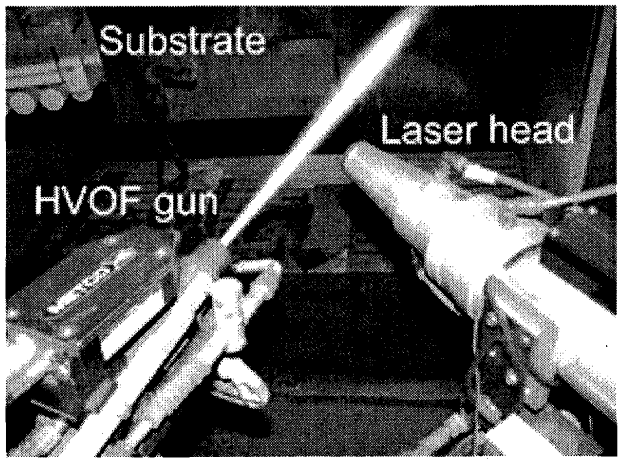

Fig.3 Photograph of hybrid spraying system.

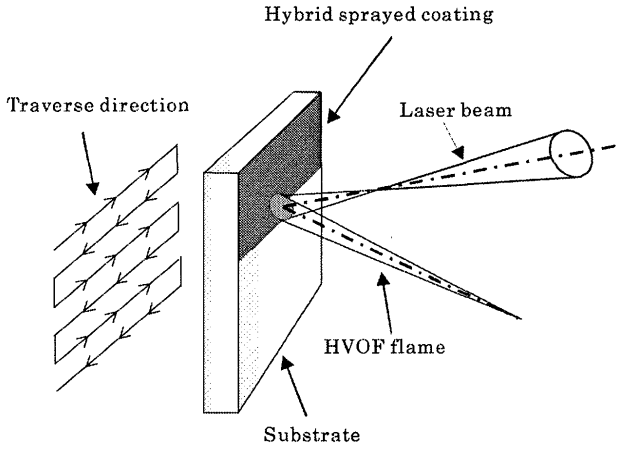

Fig.4 Schematic diagram of hybrid spraying system.

programmed so that the crosswise point of thermal spraying and laser beam are moving in a ladder shaped path on the test piece. Thermal spraying was executed by adjusting the pass number to get the required coating

thickness of 200μm automatically.

In the process of hybrid thermal spray coating, three output laser power modes of 1.5kW, 2.0kW, and 2.5kW were used (Hereinafter the coating made by 1.5kW output power as an example is referred to - "1.5 hybrid coating") and laser beam was defocused at 0, +30, +60, +90mm distance from the positive focus position to change the energy density.

For referencing purpose, another thermal spray coating that did not receive simultaneous laser irradiation was prepared (In order to identify the difference, the thermal spraying process that does not accompany laser irradiation is hereinafter referred to as HVOF thermal spray coating).

2.3 Splat collection method

In order to investigate a coating formation mechanism, it is very important to observe splat shape. Therefore, splat collection was performed in this research. **Fig.5** shows schematic diagram of the splat collection method of hybrid spraying. Cr_3C_2-Ni-Cr and pure nickel powders were used as spray materials and the polished SUS304 substrate (35mm x 35mm x 5mm) was fixed on the sample holder mounted on a six axis multiarticular robot at the crosswise point of laser and flame. On the laser head side, the hole diameter was 30mm and the hole diameter was 2mm on the HVOF gun side. Furthermore, a mask with a diameter of 30mm is installed in front of the sample holder on the HVOF gun side. The sample holder was moved upwards by the six axis multiarticular robot. While the hole of a sample holder and the hole of a mask were overlapped, so that spray particles could reach substrate.

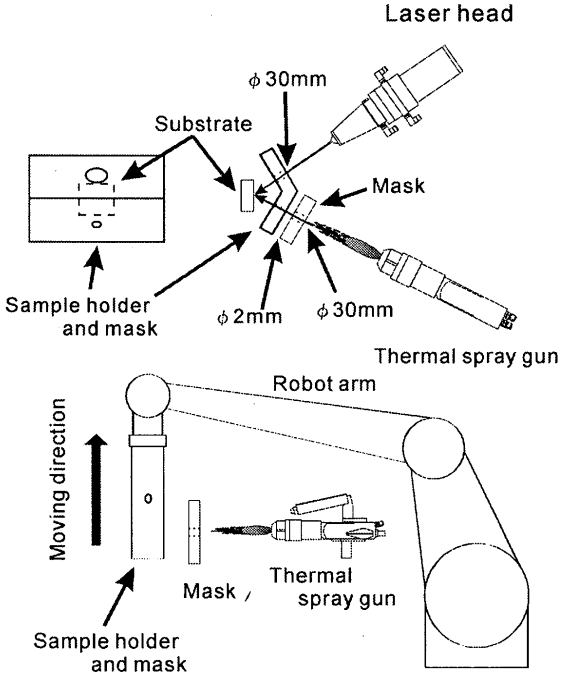

Fig.5 Schematic diagram of splat collecting aparatus method.
(a) Equipment appearance, (b) mounting arrangement of sample holder to the robot.

2.4 Evaluation method

The test piece was cut by a precise cutting machine and its surface was ground by an automatic grinder. Etching process was implemented using the Murakami reagent for the observation of coating structure before observation and analyzing of the coating structure. An EPMA system (made by JEOL Ltd. Model JXA-8900M) as well as X-ray diffraction device (made by Rigaku Electric, Model RINT-2500) were used for the composition analysis. For the measurement of coating hardness, a micro vickers hardness tester (made by Akashi Co., Model MVK-H100A2) was used under the load of 1.96N and holding duration of 15sec. Measurement was made in ten sections and average value was adopted.

A blast erosion test was also implemented conducted the Arata type coating tester[8], which is a testing device to evaluate cohesive strength of coating particles by measuring the mass change caused by drop-off of coating particles pulled out by the blasting material. As the blasting material alumina of grain size 305μm (#54) is used in one blasting shot of 70g, which was propelled by a compressed air flow of 260kPa pressure ata flow rate of 350L/min with a 30 degrees shot blasting angle. By weighins the test piece after receiving each blast shot, an average wear-out decrease out and wear-out solid volume could be calculated and expressed as a wear-out rate [8]. The equation is shown as (2.1).

$$Mv = \frac{W_1}{p \times W_2} \quad \cdots(2.1)$$

Mv:wear rate, W_1:weight loss of coating,
W_2: abrasive weight, p:coating density

3. Results

3.1 Microstructure of hybrid sprayed coatings

Fig.6 shows the back scattering electron images of

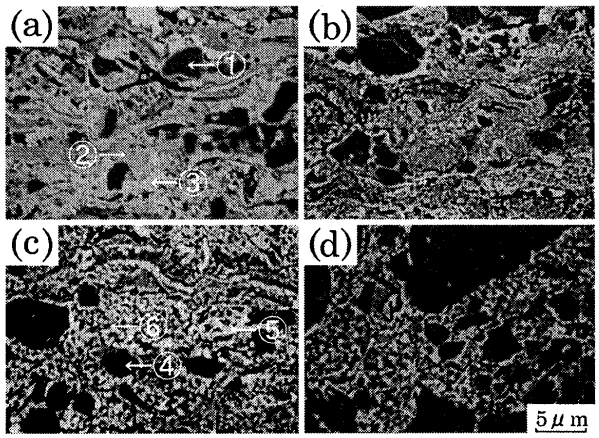

Fig.6 Back scattering electron images of cross section of hybrid spraying coatings.
(a)HVOF spraying, (b)-(d)Hybrid spraying
laser power; (b):1.5kW, (c):2.0kW, (d):2.5kW

Table 2 Results of EPMA analysis.

Position		X-ray Intensity (cps)		
		C-K α	Ni-K α	Cr-K α
Fig.6 (a)	①	410	0	220
	②	160	160	140
	③	40	360	60
Fig.6 (c)	④	410	0	190
	⑤	60	340	60
	⑥	200	160	140
Fig.7 (d)	⑦	420	0	200
	⑧	80	360	40
	⑨	230	120	170

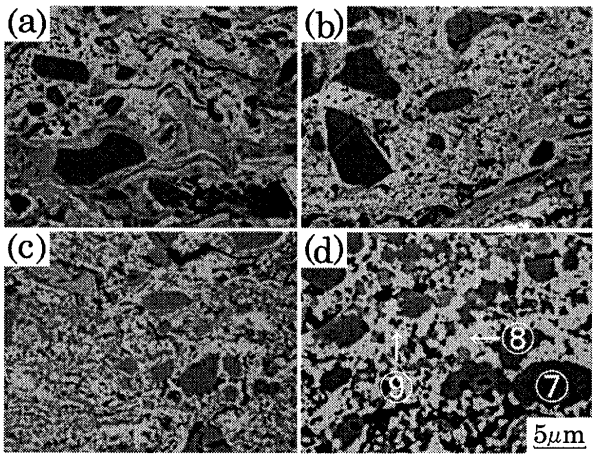

Fig.7 Back scattering electron images of cross section of HVOF coatings after heat treatment.
(a):673K, (b):873K, (c):1073K, (d):1273K

cross sections of Cr_3C_2-Ni-Cr coatings sprayed by the hybrid spray method and the HVOF spray without laser. The average micro vickers hardness of the Cr_3C_2-Ni-Cr coating with HVOF spray coating indicated 791 while that of the 1.5 hybrid coating and the 2.0 hybrid coating indicated 878 and 870 respectively. However, the hardness of the 2.5 hybrid coating showed minor reductions.

The lamellar structure that is peculiar to spray coating method is observed on the HVOF spray coating. In the matrix structure, other than of chrome carbide, there can be observed different gray scale-shades structures depending on the section. The lamellar structure was not clearly apparent on the hybrid spray coating. In this observation it was found that there are no structures in the HVOF spray coating, but many fine precipitation particles of the size about 1μm were observed, besides comparatively large sized carbide particles.

The measurement results of characteristic X-ray strengths of carbon, nickel and chrome indicated by the arrow marking in **Fig.6** and **Fig.7**, measured by EPMA are indicated in **Table 2**, that is detailed afterward. The EPMA analysis result indicated that the strength of X-ray

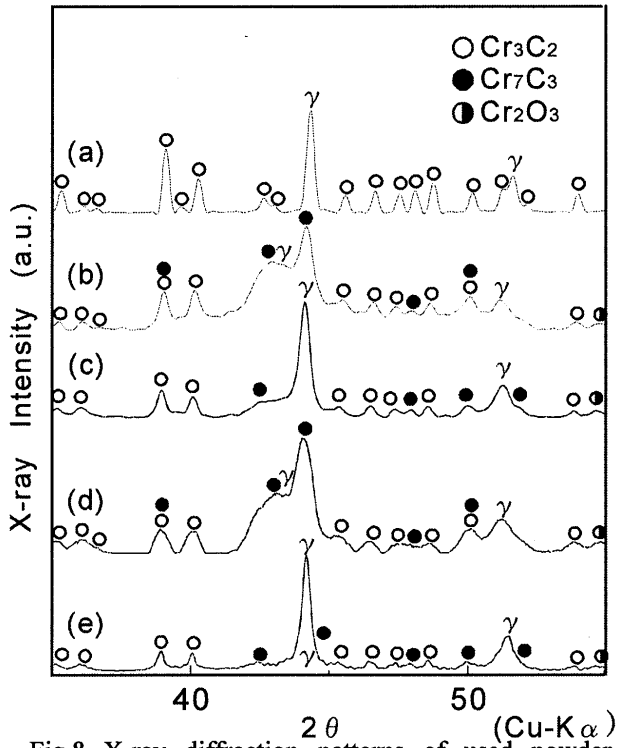

Fig.8 X-ray diffraction patterns of used powder and Cr_3C_2-Ni-Cr coatings.
(a)used powder, (b)HVOF spraying, (c)Hybrid spraying(laser power 1.5kW),
(d)-(e)heat treatment coatings, (d):673K, (e):873K

of nickel indicates higher figure in the brighter section but the darker shaded portion of black colored precipitation particles indicates a lower figure of X-ray strength in nickel and higher figures for carbon and chrome.

3.2Structural change of spray coating affected by heat treatment

Fig.7 shows the back scattering electron images of the cross sections of the sprayed coating matrix, which received heat treatment. In this image can be observed a lamellar structure which is peculiar to the spray coated layer and pores in the coating (a), which received heat-treatment made at 673K.

However, various light and dark monochrome coating structures are observed within the matrix and no large difference from the non-heat-treated matrix is recognized. Compare with this, in the coating matrix structures ((b)~(d)) that have been processed at 873K or higher temperature, it is observed neither stronger lamellar structure nor various light and dark monochrome coating structures in the matrix, but only fine precipitation objects are found. These precipitation objects gradually become larger in size when the processing temperature is increased. From the EPMA analysis result of (d) ⑦~⑨ shown in the **Table 2**, it is clearly identified that the lighter monochrome section of

the matrix contains abundant nickel and the darker section contains a lot of chrome.

Next, the X-ray diffraction patterns of spray coatings are shown in **Fig.8**, in which the result of thermal spray material is also indicated for comparison purposes. Compared with the diffraction result of thermal spray material powder, the HVOF spray coating has a lower peak of Cr_3C_2 and broader peak of γ- phase. Furthermore, the position of γ- phase peaks is shifted to a lower angled side compared with the peak positions of thermal spray material and hybrid coating [9].

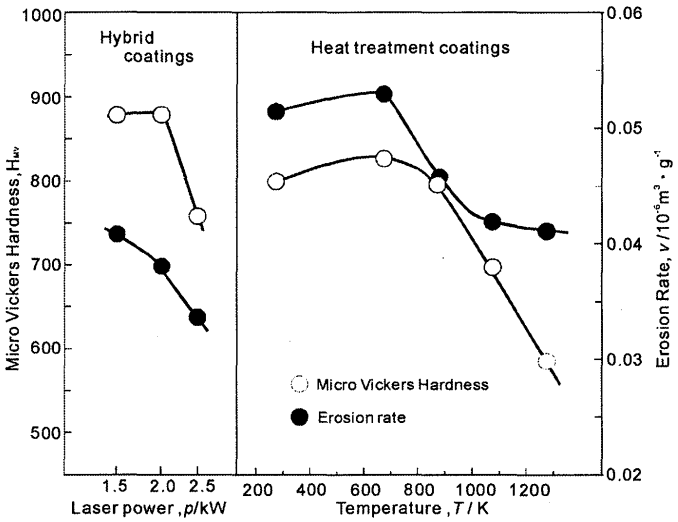

Fig.9 Results of micro vickers hardness test and blast erosion test.

On the other hand by carefully examining the result of the heat-treated coating, it can be noticed that a broader peak is observed on the coating which has been processed by 673K and which did not have any change of its coating structure in **Fig.7**, but the peak of γ-phase which had been broader now becomes sharp.

In this way, a big difference appears in the diffraction pattern and the cause of this is suggested as follows.

That is, the γ- phase dissolves chrome and the lattice constant becomes larger as the dissolved mass of chrome increases [10]. It is also considered that the γ-phase becomes a supersaturated solution including chrome and carbon of various densities because thermal spray coating particles that impact with the substrate are cooled quickly when the spray process of single HVOF spray coating is executed [11].

This means that a broader peak appears through supersaturated solution of various densities caused by the fact that the dissolution amount of chrome and/or carbon into nickel(chrome) solid solution in the γ- phase increases and rapidly cools down. The fine chrome carbide shown in **Fig.7** (b)~(d) is considered to be

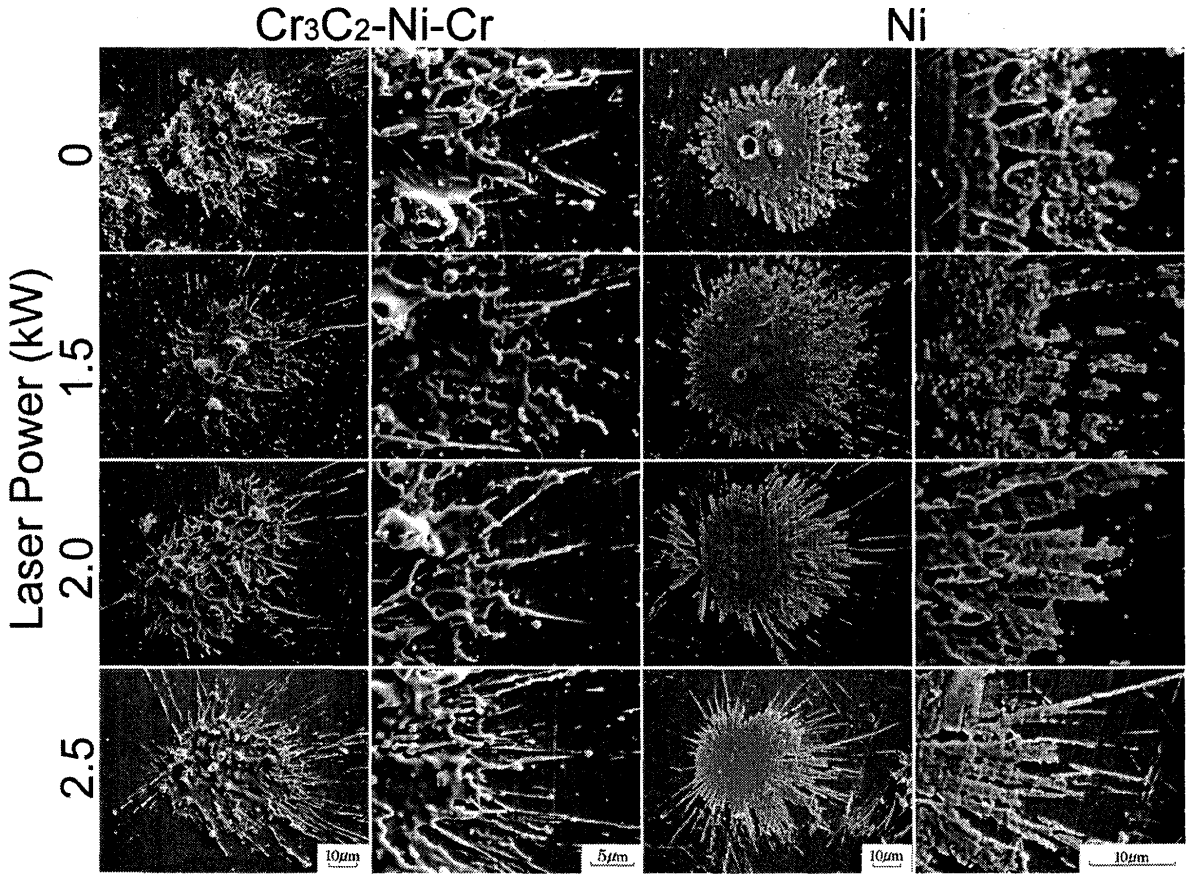

Fig.10 SEM photographs of splat particles.

precipitated from this supersaturated solid solution.

Regarding the result of X-ray diffraction of the hybrid spray coating, there is observed no broad peak in the X-ray diffraction result of the heat-treated coating processed at a temperature of higher than 873K. This clearly proves that the laser irradiation has an absolute thermal effect and this is effective in precipitating fine carbide from the supersaturated solution containing chrome and carbon.

3.3Results of micro vickers hardness test and blast erosion test of Cr_3C_2-Ni-Cr coating

Fig.9 shows micro vickers hardness and the blast erosion test results obtained from hybrid spray coatings and from the heat-treated coating. The figure of micro vickers hardness decreased rapidly in the temperature range exceeding 873K though it shows slight increase with the rise of heat-treatment temperature to 700K.

In the blast erosion test, both the 1.5 hybrid coating and the 2.0 hybrid coating indicated higher hardness values than that of the HVOF coating, but the 2.5 hybrid coating indicated a lower value. In the heat treatment coatings, no large variation of the wear-out loss can be observed under heat-treatment temperatures lower than 673K, but the abrasion loss shows a remarkable decrease in the temperature ranges exceeding 873K. Moreover, the wear-out loss of the hybrid spray coating shows a smaller value than that of the HVOF spray coating and that of the 1.5 hybrid spray coating is almost equal to the value of the heat-treated coating processed at 1273K.

The wear-out velocity of hybrid spray coatings decreased the increasing of laser output power. It is considered that the bonding strength between particles of this case has been strengthened by mutual diffusion in the coating caused by heat-treatment because the bonding strength between particles in the coating has a great influence on blast erosion loss [12-13].

According to above results, it was concluded that the hybrid coating under optimum irradiation laser power can precipitate fine chrome carbide in the coating and then strengthen the bonding strength between particles of the coating.

It is estimated that the thermal history of the coating accumulation of hybrid coating and that of the HVOF spray coating might be different due to the effect of simultaneous laser irradiation, because the coating structure of the both coatings are different. To clarify the cause of this phenomenon, an evaluation was carried out by observing the splat shape sprayed by HVOF and hybrid spraying.

3.4Effect of laser irradiation on splat shape and mechanism of coating strengthening in hybrid spraying

Fig.10 shows typical SEM photographs and shapes of splats prepared by hybrid spraying and HVOF spraying. Splat shape of HVOF spraying was mainly circular. The edge of splats sprayed by hybrid spraying was different with the laser irradiations. Hybrid spraying

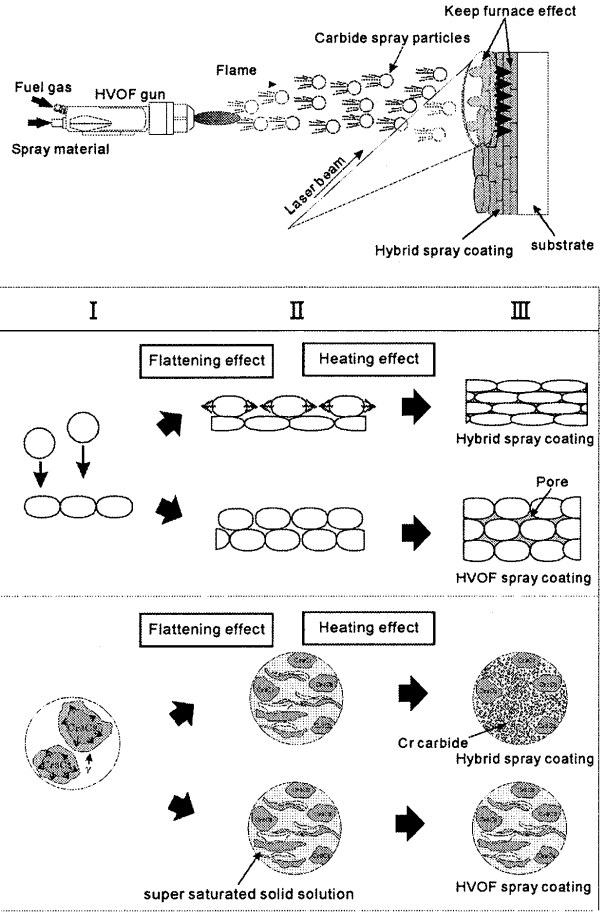

Fig.11 Schematic diagram of particle behavior in thermal spray process.

splats were more flattened in comparison with HVOF spraying splats. It is considered that the laser irradiation affects only spray particle temperature when spray particle impact on the substrate. Therefore the difference of the splat shape was caused by heating history during forming the coatings [14].

Fig.11 shows the schematic diagram of a mechanism of coating strengthening in hybrid spraying. The spray particles were heated by flame and impacted spray particles sprayed by HVOF spraying were cooled rapidly. It is considered that impacted hybrid spray particles were not cooled rapidly due to laser irradiation (named "keep furnace effect") and the splat shape became more flattened than the HVOF sprayed one. Therefore there were γ phases included in super-saturated solid solution in the Cr_3C_2-Ni-Cr HVOF sprayed coating. On the other hand there were many fine carbide particles deposited from super saturated solid solution in hybrid sprayed Cr_3C_2-Ni-Cr coatings. The porosity in hybrid sprayed coatings decreases with increasing laser output and the degree of cohesion between particles is strengthened. It was concluded that these effects improved the abrasion resistance of coatings.

4. Conclusions

In this study, the hybrid thermal spray technique, which is the laser irradiation assisted HVOF thermal spray, was applied to deposit Cr_3C_2-Ni-Cr coatings and the influence of laser assistance to the coating properties was examined. Results are as follows.

(1) Higher value of micro vickers hardness of coating prepared by laser assisted hybrid thermal spray were obtained compared to those in conventional HVOF thermal spray coatings.
(2) In the blast erosion test, the wear-out velocity of the hybrid spray coating was lower than that of the HVOF spray coating.
(3) It is considered that the improvement of micro vickers hardness of the Cr_3C_2-Ni-Cr hybrid sprayed coating resulted from the precipitation of fine chrome carbide in the matrix and its strengthening effect on cohesive strength between lamella in the coating.
(4) The splat shape sprayed by hybrid spraying was more flattened in comparison with HVOF sprayed splat. Mechanism of coating strengthening in hybrid spraying was caused by strengthening of cohesiveness by heating effects and decreasing of porosity by flattening effects.

References

1) C.J.Li, A.Ohmori and Y.Harada: Journal of Thermal Spray Technology , 5-1 (1996) 69-73.
2) CHANG-JIU LI, A.OHMORI and Y.HARADA: JOURNAL OF MATERIALS SCIENCE, 31(1996) 785-794.
3) C.-J.Li, Y.Y.Wang, T.Wu, G.C.Ji and A.Ohmori: Surface and Coatings Technology, 145(2001) 113-120.
4) M.Umagome, K.Ishikawa, G.Ueno, R.Sumita, T.Tajiri, K.Tanaka and K.Tani: Yousha gijutu manual, Japanese Standards Association , Tokyo(1998) 85-109.
5) S.Isa et al., Yousha gijutsu handbook: Shingijutu kaihatsu center,Tokyo(1998) 493-498.
6) T.Kuwashima, I.Takahashi, T.Tomita and A.Ohmori: JOURNAL OF HIGH TEMPERATURE SOCIETY 27 Supplement(2001) 269-273.
7) S.Isa et al., Yousha gijutsu handbook: Shingijutu kaihatsu center,Tokyo(1998) 180-189.
8) C.J.Li , A.Ohmori , R.Nagayama and Y.Arata: Preprints of the National Meeting of JWS.39(1986) 244.
9) W.B.Pearson: Hand book of Lattice Spacing and Structure of Metal, Pergamon Press, London(1958) 553
10) T.Tomita, Y.Takatani, K.Tani and Y.Harada: JOURNAL OF HIGH TEMPERATURE SOCIETY 26 Supplement(2000) 248-253.
11) Y.Murata , J.Takauchi, Y.Harada, T.Tomita, T.Kure and S.Nakahira: J. Japan Inst. Metals 63(1999) 126-134.
12) R.Okada, Y.Yamada: J. Japan Inst. Metals, 58-7(1994) 763-767.
13) R.Okada,K.Taguchi, K.Niikura, T.Yoshikawa: Trans. Jpn. Soc. Mech. Eng., 63-612 (1997) 197-201.
14) M.Fukumoto, H.Hayashi, T.Yokoyama: Jarnal of Japan Thermal Spraying Society, 32-3(1995) 29-36.